

# Creation of particle-hole superposition states in graphene at multiphoton resonant excitation by laser radiation

H.K. Avetissian,\* A.K. Avetissian, G.F. Mkrtchian, and Kh.V. Sedrakian

*Centre of Strong Fields Physics, Yerevan State University, 1 A. Manukian, Yerevan 0025, Armenia*

(Dated: November 10, 2018)

Nonlinear dynamics of establishment of electron-hole coherent superpositions states in graphene by multiphoton resonant excitation of interband transitions in laser fields is considered. The single-particle time dependent density matrix for such a quantized system is calculated in the multiphoton resonant approximation. The dependence of Rabi oscillations of Fermi-Dirac sea in graphene on the time, momentum, and photon number at multiphoton laser-excitation is analyzed.

PACS numbers: 78.67.Wj, 42.50.Hz, 78.47.jh, 03.65.Pm

## I. INTRODUCTION

Graphene, a single sheet of carbon atoms in a honeycomb lattice has attracted enormous interest since its experimental discovery and isolation.<sup>1,2</sup> Its quasi-particle states behave like massless “relativistic” Dirac fermions<sup>3,4</sup> and obey a two-dimensional Dirac equation, where the light speed is replaced by the Fermi velocity that is 300 times smaller than speed of light in vacuum. Beside various applications in electronic devices, graphene physics opens wide research field unifying low-energy condensed matter physics and quantum electrodynamics (QED).<sup>5-9</sup> Many fundamental nonlinear QED processes, specifically, electron-positron pair production in superstrong laser fields of ultrarelativistic intensities,<sup>10</sup> observation of which is problematic yet even in the current superintense laser fields, have their counterparts in graphene where considerably weaker electromagnetic fields are required for experimental realization of “anti-matter” production from vacuum. In this connection one can note Klein paradox,<sup>11-13</sup> Schwinger mechanism<sup>18-20</sup> and Zitterbewegung<sup>14-16</sup> for particle-hole excitation, as well as diverse physical and applied effects based on Zitterbewegung, e.g., minimal conductivity at vanishing carrier concentration<sup>21,22</sup> etc.

Due to massless energy spectrum the Compton wavelength for graphene quasiparticle tends to infinity. On the other hand, in QED the Compton wavelength is characteristic length for particle-antiparticle pair creation and annihilation. So, at the interaction of an electromagnetic field with an intrinsic graphene there is not a quasiclassical limit, since no matter how weak the applied field is and how small the photon energy is, the particle-hole pairs will be created during the whole interaction process - at arbitrary distances.

In graphene wave-particle interaction can be characterized by the dimensionless parameter

$$\chi = \frac{eE v_F}{\omega} \frac{1}{\hbar\omega},$$

which represents the work of the wave electric field  $E$  on a period  $1/\omega$  in the units of photon energy  $\varepsilon_\gamma = \hbar\omega$ . Here  $v_F$  is the Fermi velocity:  $v_F \approx c/300$ , and  $e$  is the

elementary charge. The average intensity of the wave expressed by  $\chi$ , can be estimated as:

$$I_\chi = \chi^2 \times 3.07 \times 10^{11} \text{ W cm}^{-2} [\hbar\omega/\text{eV}]^4.$$

Depending on the value of this parameter  $\chi$ , one can distinguish three different regimes in the wave-particle interaction process. Thus,  $\chi \ll 1$  corresponds to one-photon interaction regime,  $\chi \sim 1$  – to multiphoton interaction regime, and  $\chi \gg 1$  corresponds to static field limit or Schwinger regime. As is seen, the intensity  $I_\chi$  strongly depends on the photon energy. Particularly, for infrared photons:  $\varepsilon_\gamma \sim 0.1$  eV, multiphoton interaction regime can be achieved at the intensities  $I_\chi = 3.07 \times 10^7 \text{ W cm}^{-2}$ . Note that in case of free electrons at the same photon energies multiphoton effects take place at the intensities  $I \sim 10^{16} \text{ W cm}^{-2}$ .<sup>10</sup> Such a huge difference, as well as the gapless particle-hole energy spectrum in graphene makes realistic another interesting nonlinear QED process: multiphoton excitation of Dirac vacuum with Rabi oscillations at ultrafast excitation.<sup>23</sup>

In the present work the creation of particle-hole coupled states in graphene via multiphoton resonant excitation by laser fields is studied. It is well known that Rabi oscillation of states' populations is the coherent response of two-level atomic systems under resonant excitation. The one-photon resonant excitation of atoms and associated Rabi oscillations have been comprehensively studied both theoretically and experimentally and described in numerous review articles and books (see, e.g.,<sup>24</sup>). Similar phenomena have also been observed in semiconductors.<sup>25</sup> Recently, the Rabi oscillations in graphene at one-photon interband excitation (at  $\chi \ll 1$ ) and its influence on the dynamic conductivity were investigated in Refs. [26–28]. On the other hand, at a wave-particle interaction in graphene due to free-free intraband transitions we have a situation analogous to resonant excitation of quantum systems with permanent dipole moments, where direct multiphoton transitions are very effective.<sup>29-31</sup> Hence, it is of interest the creation of particle-hole coupled states in graphene via multiphoton resonant excitation. This process apart from fundamental interest may also have practical applications. In particular, particle-hole annihilation from coherent superposition states will cause

intense coherent radiation of harmonics of the applied wave-field. We consider multiphoton interaction regime at  $\chi \sim 1$ . Accordingly, the time evolution of considered process is found using a nonperturbative resonant approach arising from the quantum kinetic equations.

The paper is organized as follows. In Sec. II the set of equations for single-particle density matrix is formulated. In Sec. III we present the solution of those equations in the multiphoton resonant approximation. In Sec. IV the results of corresponding numerical simulations are presented. Finally, conclusions are given in Sec. V.

## II. BASIC MODEL AND EVOLUTIONARY EQUATION FOR SINGLE-PARTICLE DENSITY MATRIX

Let graphene interacts with a plane quasimonochromatic laser radiation of carrier frequency  $\omega$  and slowly varying envelope. To clarify the picture of stated in this paper problem for creation of coherent superposition states, we consider the case of interaction when the laser wave propagates in perpendicular direction to graphene plane ( $XY$ ) to exclude the effect of magnetic field. This travelling wave for electrons in graphene becomes a homogeneous time-periodic electric field. Let it to be directed along the  $X$ -axis with the form (constant phase connected with the position of the wave pulse maximum with respect to graphene plane is set zero):

$$\mathbf{E}(t) = \hat{x}E_0 \cos \omega t. \quad (1)$$

The problem that we attempt to solve in the given field approximation is analogous to Rabi oscillations in two level atomic systems with permanent dipole moments. In this case, the physical picture of resonant wave-graphene interaction will be more transparent in the length gauge. So, for the interaction Hamiltonian we will use length gauge describing the interaction by the potential energy. Cast in the second quantization formalism, the Hamiltonian is

$$\hat{H} = \int \hat{\Psi}^\dagger \hat{H}_s \hat{\Psi} dx dy, \quad (2)$$

where  $\hat{\Psi}$  is the fermionic field operator,  $\hat{H}_s$  is the single-particle Hamiltonian in the external homogeneous electric field (1). Omitting here real spin and valley quantum numbers, single-particle Hamiltonian can be written as:

$$\hat{H}_s = v_F \begin{pmatrix} 0 & \hat{p}_x - i\hat{p}_y \\ \hat{p}_x + i\hat{p}_y & 0 \end{pmatrix} + \begin{pmatrix} exE & 0 \\ 0 & exE \end{pmatrix}, \quad (3)$$

where  $v_F \approx c/300$  is the Fermi velocity ( $c$  is the light speed in vacuum),  $\hat{\mathbf{p}} = \{\hat{p}_x, \hat{p}_y\}$  is the electron momentum operator. The first term in (3) is the Hamiltonian of two-dimensional massless Dirac fermion and the second term is the interaction part.

We write the fermionic field operator in the form of an expansion in the free Dirac states:

$$\hat{\Psi}(x, y, t) = \sum_{\mathbf{p}, \sigma} \hat{a}_{\mathbf{p}, \sigma}(t) \Psi_{\mathbf{p}, \sigma}(x, y), \quad (4)$$

where the creation and annihilation operators,  $\hat{a}_{\mathbf{p}, \sigma}^\dagger(t)$  and  $\hat{a}_{\mathbf{p}, \sigma}(t)$ , associated with positive ( $\sigma = 1$ ) and negative ( $\sigma = -1$ ) energy solutions satisfy the anticommutation rules at equal times

$$\{\hat{a}_{\mathbf{p}, \sigma}^\dagger(t), \hat{a}_{\mathbf{p}', \sigma'}(t')\}_{t=t'} = \delta_{\mathbf{p}, \mathbf{p}'} \delta_{\sigma, \sigma'}, \quad (5)$$

$$\{\hat{a}_{\mathbf{p}, \sigma}^\dagger(t), \hat{a}_{\mathbf{p}', \sigma'}^\dagger(t')\}_{t=t'} = \{\hat{a}_{\mathbf{p}, \sigma}(t), \hat{a}_{\mathbf{p}', \sigma'}(t')\}_{t=t'} = 0. \quad (6)$$

The free Dirac solutions corresponding to energies  $\mathcal{E}_\sigma = \sigma v_F \sqrt{p_x^2 + p_y^2}$  ( $\sigma = \pm 1$ ) are:

$$\Psi_{\mathbf{p}, \sigma}(x, y) = \frac{1}{\sqrt{2S}} \begin{pmatrix} 1 \\ \sigma e^{i\Theta(\mathbf{p})} \end{pmatrix} e^{\frac{i}{\hbar}(p_x x + p_y y)}, \quad (7)$$

where  $S$  is the quantization area (graphene layer surface area) and

$$\Theta(\mathbf{p}) = \arctan\left(\frac{p_y}{p_x}\right) \quad (8)$$

is the angle in momentum space.

Taking into account Eqs. (1)-(8), the second quantized Hamiltonian can be expressed in the form:

$$\begin{aligned} \hat{H} &= \sum_{\mathbf{p}, \sigma} \mathcal{E}_\sigma(p) \hat{a}_{\mathbf{p}, \sigma}^\dagger \hat{a}_{\mathbf{p}, \sigma} \\ &+ eE(t) \sum_{\mathbf{p}, \sigma} \sum_{\mathbf{p}', \sigma'} D_{\sigma\sigma'}(\mathbf{p}, \mathbf{p}') \hat{a}_{\mathbf{p}, \sigma}^\dagger \hat{a}_{\mathbf{p}', \sigma'}, \end{aligned} \quad (9)$$

where

$$\begin{aligned} D_{\sigma\sigma'}(\mathbf{p}, \mathbf{p}') &= \frac{1}{2S} \left[ 1 + \sigma\sigma' e^{i(\Theta(\mathbf{p}') - \Theta(\mathbf{p}))} \right] \\ &\times \int x e^{\frac{i}{\hbar}(\mathbf{p}' - \mathbf{p})\mathbf{r}} dx dy. \end{aligned} \quad (10)$$

We will use Heisenberg representation, where operators evolution are given by the following equation:

$$i\hbar \frac{\partial \hat{L}}{\partial t} = [\hat{L}, \hat{H}], \quad (11)$$

and expectation values are determined by the initial density matrix  $\hat{D}$ :

$$\langle \hat{L} \rangle = \text{Sp}(\hat{D}\hat{L}). \quad (12)$$

The single-particle density matrix in momentum space is defined as:

$$\rho_{\sigma_1 \sigma_2}(\mathbf{p}_1, \mathbf{p}_2, t) = \langle \hat{a}_{\mathbf{p}_2, \sigma_2}^\dagger(t) \hat{a}_{\mathbf{p}_1, \sigma_1}(t) \rangle. \quad (13)$$

For initial state of graphene quasiparticles we assume ideal Fermi gas in equilibrium. This means that the initial single-particle density matrix is diagonal and we have Fermi-Dirac distribution:

$$\rho_{\sigma\sigma'}(\mathbf{p}, \mathbf{p}', 0) = \frac{1}{1 + e^{\frac{\mathcal{E}_\sigma(\mathbf{p}) - \mu}{T}}} \delta_{\mathbf{p}, \mathbf{p}'} \delta_{\sigma, \sigma'}. \quad (14)$$

Here  $\mu$  is the chemical potential,  $T$  is the temperature in energy units. Taking into account definition (13), from Eq. (11) one can obtain evolution equation for single-particle density matrix:

$$\begin{aligned} i\hbar \frac{\partial \rho_{\sigma_1 \sigma_2}(\mathbf{p}_1, \mathbf{p}_2, t)}{\partial t} &= [\mathcal{E}_{\sigma_1}(p_1) - \mathcal{E}_{\sigma_2}(p_2)] \rho_{\sigma_1 \sigma_2}(\mathbf{p}_1, \mathbf{p}_2, t) \\ &- eE(t) \sum_{\mathbf{p}, \sigma} [D_{\sigma\sigma_2}(\mathbf{p}, \mathbf{p}_2) \rho_{\sigma_1 \sigma}(\mathbf{p}_1, \mathbf{p}, t) \\ &- D_{\sigma_1 \sigma}(\mathbf{p}_1, \mathbf{p}) \rho_{\sigma\sigma_2}(\mathbf{p}, \mathbf{p}_2, t)]. \end{aligned} \quad (15)$$

Then taking into account the following relation with Dirac delta function  $\delta(\alpha)$ :

$$\int_{-\infty}^{\infty} x e^{-i\alpha x} dx = 2\pi i \frac{\partial}{\partial \alpha} \delta(\alpha)$$

and substitution

$$\sum_{\mathbf{p}} \rightarrow \frac{S}{(2\pi\hbar)^2} \int d\mathbf{p},$$

we obtain closed set of equation for the density matrix elements:

$$\begin{aligned} &\left. \frac{\partial \rho_{\sigma, \sigma}(\mathbf{p}, \mathbf{p}, t)}{\partial t} - eE(t) \frac{\partial \rho_{\sigma, \sigma}(\mathbf{p}_1, \mathbf{p}, t)}{\partial p_{1x}} \right|_{\mathbf{p}_1 = \mathbf{p}} \\ &- eE(t) \left. \frac{\partial \rho_{\sigma, \sigma}(\mathbf{p}, \mathbf{p}_2, t)}{\partial p_{2x}} \right|_{\mathbf{p}_2 = \mathbf{p}} = i \frac{eE(t)}{2} \frac{\partial \Theta(\mathbf{p})}{\partial p_x} \\ &\times [\rho_{\sigma, -\sigma}(\mathbf{p}, \mathbf{p}, t) - \rho_{-\sigma, \sigma}(\mathbf{p}, \mathbf{p}, t)], \quad (16) \\ &\left. \frac{\partial \rho_{\sigma, -\sigma}(\mathbf{p}, \mathbf{p}, t)}{\partial t} - eE(t) \frac{\partial \rho_{\sigma, -\sigma}(\mathbf{p}_1, \mathbf{p}, t)}{\partial p_{1x}} \right|_{\mathbf{p}_1 = \mathbf{p}} \\ &- eE(t) \left. \frac{\partial \rho_{\sigma, -\sigma}(\mathbf{p}, \mathbf{p}_2, t)}{\partial p_{2x}} \right|_{\mathbf{p}_2 = \mathbf{p}} = \frac{2}{i\hbar} \mathcal{E}_\sigma(p) \rho_{\sigma, -\sigma}(\mathbf{p}, \mathbf{p}, t) \\ &- \frac{eE(t)}{2i} \frac{\partial \Theta(\mathbf{p})}{\partial p_x} [\rho_{\sigma, \sigma}(\mathbf{p}, \mathbf{p}, t) - \rho_{-\sigma, -\sigma}(\mathbf{p}, \mathbf{p}, t)]. \quad (17) \end{aligned}$$

In Eqs. (16) and (17) one can eliminate the terms with partial derivatives  $\partial/\partial p_x$  by the method of characteristics. The characteristic of these equations is the classical equation of motion:

$$\frac{d\mathbf{p}}{dt} = -e\mathbf{E}(t)$$

with the solution

$$p_x = p_{0x} + p_E(t); \quad p_y = p_{0y}, \quad (18)$$

where

$$p_E(t) = -e \int_0^t E(t') dt' = -\frac{eE_0}{\omega} \sin \omega t$$

is the momentum given by the wave-field. Thus, with the new variables  $p_{0x}$ ,  $p_{0y}$ , and  $t$  Eqs. (16) and (17) read:

$$\begin{aligned} \frac{\partial \rho_{\sigma, \sigma}(\mathbf{p}_0, \mathbf{p}_0, t)}{\partial t} &= \frac{i}{2} F(\mathbf{p}_0, t) \\ &\times [\rho_{\sigma, -\sigma}(\mathbf{p}_0, \mathbf{p}_0, t) - \rho_{-\sigma, \sigma}(\mathbf{p}_0, \mathbf{p}_0, t)], \quad (19) \end{aligned}$$

$$\begin{aligned} \frac{\partial \rho_{\sigma, -\sigma}(\mathbf{p}_0, \mathbf{p}_0, t)}{\partial t} &= \frac{2}{i\hbar} \tilde{\mathcal{E}}_\sigma(\mathbf{p}_0, t) \rho_{\sigma, -\sigma}(\mathbf{p}_0, \mathbf{p}_0, t) \\ &+ \frac{i}{2} F(\mathbf{p}_0, t) [\rho_{\sigma, \sigma}(\mathbf{p}_0, \mathbf{p}_0, t) - \rho_{-\sigma, -\sigma}(\mathbf{p}_0, \mathbf{p}_0, t)], \quad (20) \end{aligned}$$

where

$$F(\mathbf{p}_0, t) = -\frac{eE(t) p_{0y}}{(p_{0x} + p_E(t))^2 + p_{0y}^2} \quad (21)$$

and

$$\tilde{\mathcal{E}}_\sigma(\mathbf{p}_0, t) = \sigma v_F \sqrt{(p_{0x} + p_E(t))^2 + p_{0y}^2}. \quad (22)$$

Taking into account Eq. (18), it is easy to see that

$$\rho_{\sigma, \sigma'}(\mathbf{p}_0, \mathbf{p}_0, 0) = \rho_{\sigma, \sigma'}(\mathbf{p}, \mathbf{p}, 0). \quad (23)$$

To be more precise in the set of equations (16) and (17) one should add the terms describing relaxation processes. Since we have not taken into account the relaxation processes, this consideration is correct only for the times  $t < \tau_{\min}$ , where  $\tau_{\min}$  is the minimum of all relaxation times. Thus, full dynamics in the absence of any losses is now governed by Eqs. (19) and (20). These equations yield the conservation law for the particle number:

$$\begin{aligned} &\rho_{1,1}(\mathbf{p}_0, \mathbf{p}_0, t) + \rho_{-1,-1}(\mathbf{p}_0, \mathbf{p}_0, t) = \\ &= \rho_{1,1}(\mathbf{p}_0, \mathbf{p}_0, 0) + \rho_{-1,-1}(\mathbf{p}_0, \mathbf{p}_0, 0) \equiv \Xi(p_0, \mu, T). \quad (24) \end{aligned}$$

Here we have introduced the notation  $\Xi_{p_0, \mu, T}$ , which according to Eq. (14) is:

$$\Xi_{p_0, \mu, T} = \frac{1}{1 + e^{\frac{v_F p_0 - \mu}{T}}} + \frac{1}{1 + e^{\frac{-v_F p_0 - \mu}{T}}}.$$

In Eqs.(19) and (20) diagonal elements represent particle  $\mathcal{N}(\mathbf{p}_0, t) \equiv \rho_{1,1}(\mathbf{p}_0, \mathbf{p}_0, t)$  and hole  $(1 -$

$\rho_{-1,-1}(\mathbf{p}_0, \mathbf{p}_0, t)$  distribution functions, while nondiagonal elements  $\rho_{1,-1}(\mathbf{p}_0, \mathbf{p}_0, t) = \rho_{-1,1}^*(\mathbf{p}_0, \mathbf{p}_0, t)$  describe particle-hole coherent transitions. Introducing the new quantity ( $\mathcal{J}(\mathbf{p}_0, t)$ ):

$$\rho_{1,-1}(\mathbf{p}_0, \mathbf{p}_0, t) = i\mathcal{J}(\mathbf{p}_0, t) \exp \left\{ -i\frac{2}{\hbar} \int_0^t \tilde{\mathcal{E}}_1(\mathbf{p}_0, t') dt' \right\}$$

and taking into account that  $\rho_{-1,-1}(\mathbf{p}_0, \mathbf{p}_0, t) = \Xi_{p_0, \mu, T} - \mathcal{N}(\mathbf{p}_0, t)$ , from Eqs.(19) and (20) we obtain the following set of equations:

$$\frac{\partial \mathcal{N}(\mathbf{p}_0, t)}{\partial t} = -\frac{1}{2} F(\mathbf{p}_0, t)$$

$$\times \left[ \mathcal{J}(\mathbf{p}_0, t) \exp \left\{ -i\frac{2}{\hbar} \int_0^t \tilde{\mathcal{E}}_1(\mathbf{p}_0, t') dt' \right\} + \text{c.c.} \right], \quad (25)$$

$$\begin{aligned} \frac{\partial \mathcal{J}(\mathbf{p}_0, t)}{\partial t} &= \frac{1}{2} F(\mathbf{p}_0, t) \exp \left\{ i\frac{2}{\hbar} \int_0^t \tilde{\mathcal{E}}_1(\mathbf{p}_0, t') dt' \right\} \\ &\times [2\mathcal{N}(\mathbf{p}_0, t) - \Xi_{p_0, \mu, T}]. \end{aligned} \quad (26)$$

This set of equations should be solved with the initial conditions:

$$\mathcal{J}(\mathbf{p}_0, 0) = 0; \quad \mathcal{N}(\mathbf{p}_0, 0) = \frac{1}{1 + e^{\frac{v_F p_0 - \mu}{T}}}. \quad (27)$$

### III. MULTIPHOTON RESONANT EXCITATION

The Eqs. (25) and (26) represent linear set of equations with periodic coefficients and are analogous to Bloch equations,<sup>24</sup> which describe Rabi oscillation of states' populations of two-level atomic system under resonant excitation. Note that there are significant differences between usual Bloch equations and Eqs. (25), (26). Thus, from the Floquet theorem and Eq. (22) follows that instead of stationary levels  $v_F p_0$  and  $-v_F p_0$  due to free-free intraband transitions we have quasistationary states with quasienergies:  $\tilde{\mathcal{E}}_{\pm}(s) = \pm \mathcal{E}_{E_0}(\mathbf{p}_0) + s\omega$ ;  $s = 0, \pm 1, \pm 2, \dots$ . Here

$$\begin{aligned} \mathcal{E}_{E_0}(\mathbf{p}_0) &= \frac{\omega}{2\pi} \int_0^{2\pi/\omega} \tilde{\mathcal{E}}_1(\mathbf{p}_0, t) dt \\ &= v_F \frac{\omega}{2\pi} \int_0^{2\pi/\omega} \sqrt{\left( p_{0x} - \frac{eE_0}{\omega} \sin \omega t \right)^2 + p_{0y}^2} dt \end{aligned} \quad (28)$$

is the mean value of classical energy in the field (1), which has a nonlinear dependence on the amplitude of the wave-field. The latter in the physical sense is the dynamic Stark shift due to free-free intraband transitions. Two Floquet ladders are coupled by the term

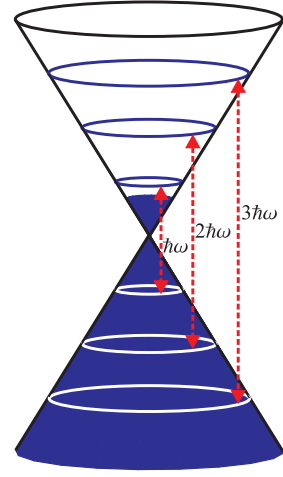


FIG. 1: Graphene conical dispersion with interband multiphoton transitions induced by external electric field.

$F(\mathbf{p}_0, t + 2\pi/\omega) = F(\mathbf{p}_0, t)$ , which in turn contains all harmonics of driving field. In usual Bloch equations coupling contains only fundamental oscillations, which provide only direct one photon resonant excitation. Situation is analogous to resonant excitation of systems with permanent dipole moments, where, as has been shown in Ref. [29], it is possible to decouple slow and rapid oscillations and to disclose the resonant dynamics of the wave-particle interaction.

Because of space homogeneity of the field (1), the generalized momentum of a particle conserves, so that the real transitions in the field occur from a  $-\mathcal{E}_{E_0}(\mathbf{p}_0)$  negative energy level to the positive  $+\mathcal{E}_{E_0}(\mathbf{p}_0)$  energy level and, consequently, the multiphoton probabilities of particle-hole pair production will have maximal values for the resonant transitions

$$2\mathcal{E}_{E_0} \simeq n\hbar\omega. \quad (29)$$

Note that the resonant condition (29) is equivalent to crossing of Floquet ladders:  $\tilde{\mathcal{E}}_-(s+n) \simeq \tilde{\mathcal{E}}_+(s)$ . Figure 1 schematically illustrates multiphoton interband transition between the two states in the filled lower cone and the empty part of upper cone. To decouple slow and rapid oscillations at the resonant condition (29), we follow the ansatz developed in Ref. [29] and represent Eqs. (25) and (26) in the form:

$$\begin{aligned} \frac{\partial \mathcal{N}(\mathbf{p}_0, t)}{\partial t} &= -\frac{1}{2} \mathcal{J}(\mathbf{p}_0, t) \\ &\times \sum_s G_s^*(\mathbf{p}_0, E_0) e^{-i\left(\frac{2}{\hbar} \mathcal{E}_E(\mathbf{p}_0) - s\omega\right)t} + \text{c.c.}, \end{aligned} \quad (30)$$

$$\begin{aligned} \frac{\partial \mathcal{J}(\mathbf{p}_0, t)}{\partial t} &= \frac{1}{2} \sum_s G_s(\mathbf{p}_0, E_0) e^{i\left(\frac{2}{\hbar} \mathcal{E}_E(\mathbf{p}_0) - s\omega\right)t} \\ &\times [2\mathcal{N}(\mathbf{p}_0, t) - \Xi_{p_0, \mu, T}]. \end{aligned} \quad (31)$$

Here  $s$  photon coupling coefficient is:

$$G_s(\mathbf{p}_0, E_0) = \frac{\omega}{2\pi} \int_0^{2\pi/\omega} F(\mathbf{p}_0, t) \times \exp \left\{ - \sum_{m \neq 0} \frac{2\mathcal{E}_m(\mathbf{p}_0)}{m\hbar\omega} e^{-im\omega t} \right\} e^{is\omega t} dt, \quad (32)$$

where

$$\mathcal{E}_m(\mathbf{p}_0) = \frac{\omega}{2\pi} \int_0^{2\pi/\omega} \tilde{\mathcal{E}}_1(\mathbf{p}_0, t) e^{im\omega t} dt. \quad (33)$$

Close to resonance (29), the main coupling term in Eqs. (30) and (31) becomes slowly varying term with  $s = n$ . The remaining nonresonant and rapidly oscillating terms are responsible only for dynamic Stark shifts.<sup>29</sup> Thus, for time average functions  $\overline{\mathcal{N}}(\mathbf{p}_0, t)$  and  $\overline{\mathcal{J}}(\mathbf{p}_0, t)$  one can obtain the following set of equations:

$$\frac{\partial \overline{\mathcal{N}}(\mathbf{p}_0, t)}{\partial t} = -\frac{1}{2} \overline{\mathcal{J}}(\mathbf{p}_0, t) G_n^*(\mathbf{p}_0, E_0) e^{-i\delta_n t} + \text{c.c.}, \quad (34)$$

$$\begin{aligned} & \frac{\partial \overline{\mathcal{J}}(\mathbf{p}_0, t)}{\partial t} + i\delta_{st} \overline{\mathcal{J}}(\mathbf{p}_0, t) \\ &= \frac{1}{2} G_n(\mathbf{p}_0, E_0) e^{i\delta_n t} (2\overline{\mathcal{N}}(\mathbf{p}_0, t) - \Xi_{p_0, \mu, T}). \end{aligned} \quad (35)$$

Here we have introduced resonance detuning

$$\delta_n = \frac{2\mathcal{E}_E(\mathbf{p}_0) - n\hbar\omega}{\hbar} \quad (36)$$

and dynamic Stark shift

$$\delta_{st} = \frac{1}{2\omega} \sum_{s \neq n} \frac{|G_s(\mathbf{p}_0, E_0)|^2}{(n-s)}. \quad (37)$$

The latter is the result of virtual nonresonant transition within Floquet states. Thus, we have a set of linear ordinary differential equations the solution of which at the initial condition (27) is:

$$\begin{aligned} \overline{\mathcal{J}}(\mathbf{p}_0, t) &= e^{i\delta_n t} \frac{G_n(\mathbf{p}_0, E_0)}{2\Omega_n} \Delta_{p_0, \mu, T} \\ &\times \left( \sin \Omega_n t - i \frac{\delta_n + \delta_{st}}{\Omega_n} (1 - \cos \Omega_n t) \right), \quad (38) \\ \overline{\mathcal{N}}(\mathbf{p}_0, t) &= \frac{\Xi_{p_0, \mu, T}}{2} + \frac{|G_n(\mathbf{p}_0, E_0)|^2}{2\Omega_n^2} \Delta_{p_0, \mu, T} \\ &\times \left[ \frac{(\delta_n + \delta_{st})^2}{|G_n(\mathbf{p}_0, E_0)|^2} + \cos \Omega_n t \right], \quad (39) \end{aligned}$$

where

$$\Delta_{p_0, \mu, T} = \frac{1}{1 + e^{\frac{\nu_F p_0 - \mu}{T}}} - \frac{1}{1 + e^{\frac{-\nu_F p_0 - \mu}{T}}} \quad (40)$$

is the initial population inversion, and

$$\Omega_n = \sqrt{|G_n(\mathbf{p}_0, E_0)|^2 + (\delta_n + \delta_{st})^2} \quad (41)$$

is the generalized Rabi frequency. The solution (39) expresses Rabi flopping among the particle-hole states at the multiphoton resonance. The solutions (38), (39) have been derived using the assumption that  $\overline{\mathcal{N}}(\mathbf{p}_0, t)$  and  $\overline{\mathcal{J}}(\mathbf{p}_0, t)$  are slowly varying functions on the scale of the wave period, which put the following restrictions:

$$(|G_n(\mathbf{p}_0, E_0)|, |\delta_n|, |\delta_{st}|) \ll \omega \quad (42)$$

on the characteristic parameters of the system considered.

For the exact resonance ( $\delta_n + \delta_{st} = 0$ ) we have  $\Omega_n = |G_n(\mathbf{p}_0, E_0)|$  and the solutions become:

$$\mathcal{J}(\mathbf{p}_0, t) = \frac{\Delta_{p_0, \mu, T}}{2} e^{i \arg(G_n(\mathbf{p}_0, E_0))} \sin \Omega_n t, \quad (43)$$

$$\mathcal{N}(\mathbf{p}_0, t) = \frac{\Delta_{p_0, \mu, T}}{2} \cos \Omega_n t + \frac{\Xi_{p_0, \mu, T}}{2}. \quad (44)$$

At one-photon interband excitation (when  $\chi_0 \ll 1$ ) (32) one can omit nonlinear over  $E_0$  terms and for Rabi frequency we have:

$$\Omega_1 = \frac{eE_0 |\sin \Theta(\mathbf{p}_0)|}{2p_0}.$$

Taking into account resonant condition  $2p_0 \nu_F \simeq \hbar\omega$ , the latter can be expressed through the interaction parameter  $\chi_0 = eE_0 \nu_F / (\hbar\omega^2)$ :

$$\Omega_1 = \omega |\sin \Theta(\mathbf{p}_0)| \chi_0.$$

With increasing of pump wave intensity, the Rabi oscillations appear corresponding to multiphoton transitions. At that one should take into account the intensity effect of the pump wave on the quasienergy spectrum (Stark shift due to free-free intraband transitions) and the dynamic Stark shift due to virtual nonresonant transitions. For  $\chi \sim 1$ , the probabilities of multiphoton transitions are essential up to photon numbers  $n \sim 5$ . For this photon numbers the Stark shift (38) is not essential, while the modification in the quasienergy spectrum is considerable. Isolines of quasienergy spectrum, defined by Eq. (28), are no longer circles but ellipse-like. In Fig. 2, isolines of quasienergy corresponding to resonant condition  $2\mathcal{E}_{E_0}(\mathbf{p}_0) / \hbar\omega \approx n$  (29) with detuning  $|\delta_n| / \omega = 0.02$ , for  $n = 2, 3, 4$  are shown in the multiphoton interaction regime:  $\chi_0 = 1$ . As is seen, modification of unperturbed

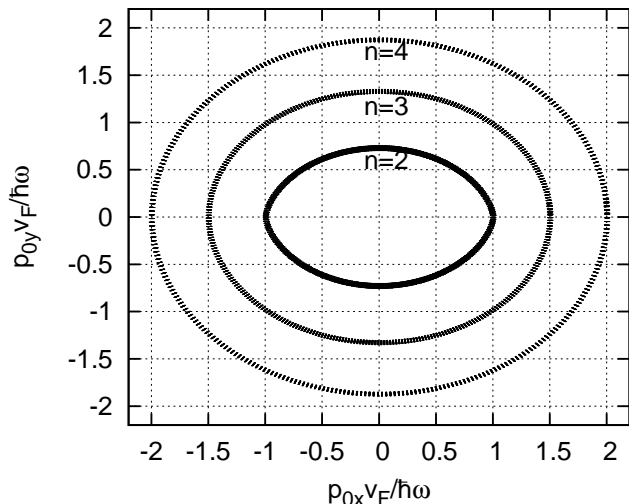


FIG. 2: Isolines of quasienergy corresponding to resonant condition  $2\mathcal{E}_{E_0}(\mathbf{p}_0)/\hbar\omega \approx n$  (29) with detuning  $|\delta_n|/\omega = 0.02$ , for  $n = 2, 3, 4$ . The electric field dimensionless parameter is taken to be  $\chi_0 = 1.0$ . The momentum components are normalized to  $\hbar\omega/v_F$ .

energy spectrum in the direction perpendicular to the electric field vector, is considerable (for example, at  $n = 3$  we have 13% deviation). Thus, in the multiphoton interaction regime one should expect photoexcitation of particle distribution function just along the modified isolines, in accordance with Eq. (44).

#### IV. NUMERICAL TREATMENT

We have also performed numerical simulations and integrated Eqs. (25) and (26) with the fourth-order adaptive Runge-Kutta method. As we mainly interested by interband multiphoton transitions, for all calculations the chemical potential and temperature are fixed and are taken to be  $\mu/\hbar\omega = 0.1$  and  $T/\hbar\omega = 5 \times 10^{-3}$ .

In Figures 3-5 photoexcitations of Fermi-Dirac sea is presented: density plot of the particle distribution function  $\mathcal{N}(\mathbf{p}_0, t)$  is shown for various pump wave intensities and instants. In Fig. 3 corresponding to  $\chi_0 = 0.02$ , we see only creation of particle-hole pair in graphene at the one-photon resonant excitation. In Fig. 4, the pump wave intensity is larger:  $\chi_0 = 0.5$  and, as a consequence, we see resonant rings corresponding to multiphoton excitation up to four photons. In Fig. 5, which corresponds to  $\chi_0 = 1$ , it is clearly seen also the ring for five photon resonance. At that, the ring for one-photon excitation is smeared, since Stark shift for this energy is comparable to  $\hbar\omega$  and the condition (42) for resonant Rabi oscillations at one-photon excitation is not fulfilled. As is seen from Figs. 4 and 5, the excitation of Fermi-Dirac sea takes place along the ellipse-like isolines of quasienergy spec-

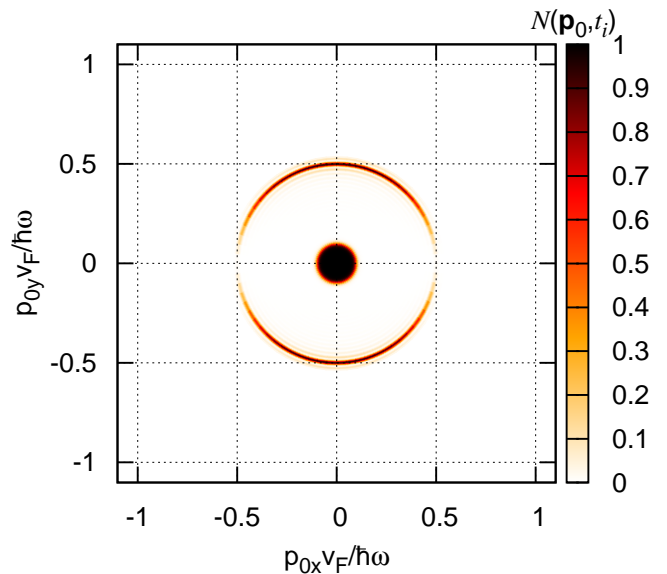


FIG. 3: (Color online) Creation of particle-hole pair in graphene at the one-photon resonant excitation. Particle distribution function  $\mathcal{N}(\mathbf{p}_0, t)$  (in arbitrary units) at instant  $t_i = 25\mathcal{T}$ , as a function of scaled dimensionless momentum components  $\{p_{0x}v_F/\hbar\omega, p_{0y}v_F/\hbar\omega\}$ . The electric field dimensionless parameter is  $\chi_0 = 0.02$ .

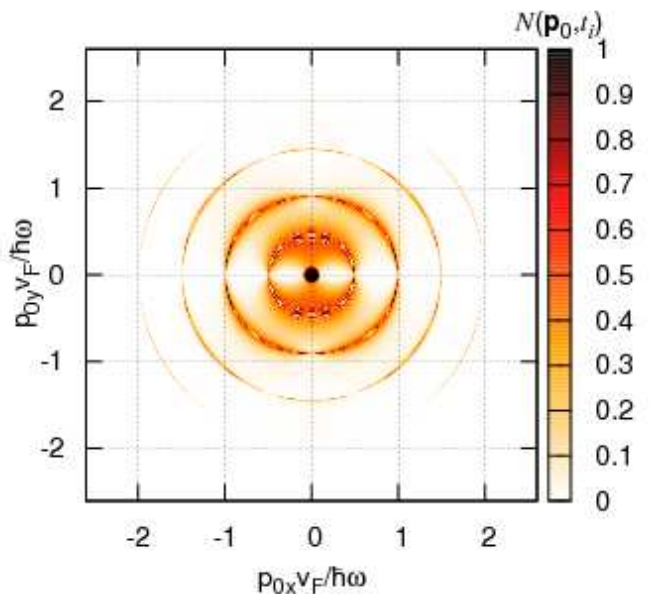


FIG. 4: (Color online) Creation of particle-hole pair in graphene at the multiphoton resonant excitation. Particle distribution function  $\mathcal{N}(\mathbf{p}_0, t)$  (in arbitrary units) at instant  $t_i = 100\mathcal{T}$ , as a function of scaled dimensionless momentum components  $\{p_{0x}v_F/\hbar\omega, p_{0y}v_F/\hbar\omega\}$ . The electric field dimensionless parameter is  $\chi_0 = 0.5$ .

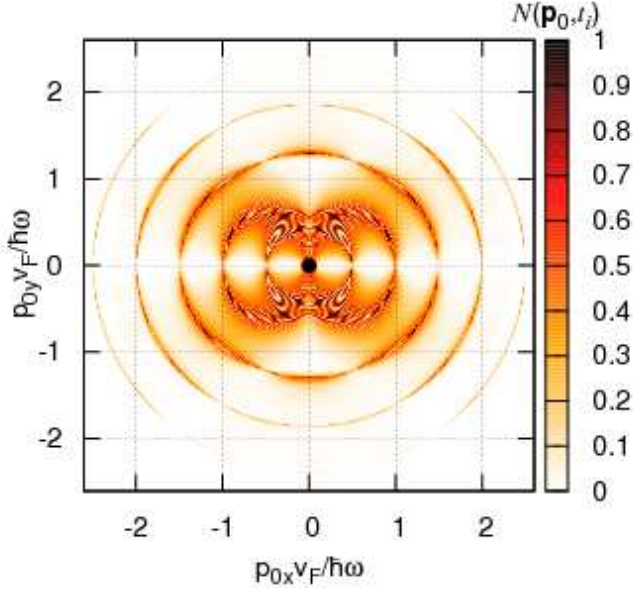


FIG. 5: (Color online) Same as Fig. 4, but for stronger wave-field with  $\chi_0 = 1$ .

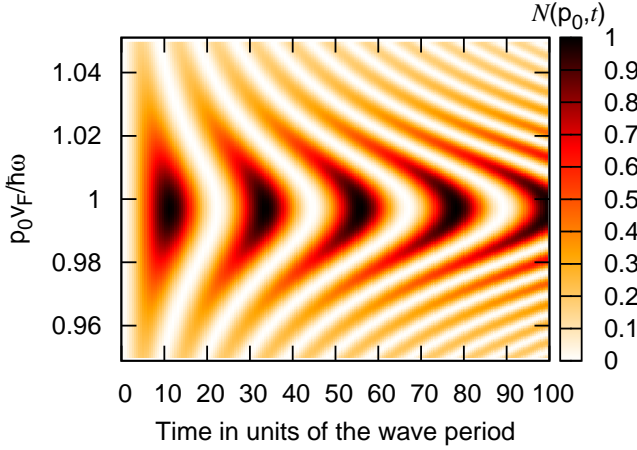


FIG. 6: (Color online) Two-photon resonance ( $n = 2$ ). Rabi oscillations of the particle distribution function  $\mathcal{N}(p_0, t)$  for the fixed angle  $\Theta(\mathbf{p}_0) = 0.2$  rad versus the scaled dimensionless momentum  $p_{0y} v_F / \hbar \omega$ . The electric field dimensionless parameter is  $\chi_0 = 0.5$ .

trum defined by Eq. (28), in accordance with analytical treatment (see, Fig. 2).

To show the dynamics of multiphoton excitation of Fermi-Dirac sea in Figs. 6-8, we present Rabi oscillations of the particle distribution function  $\mathcal{N}(p_0, t)$  for the fixed angles versus the scaled dimensionless momentum  $p_{0y} v_F / \hbar \omega$ . Figure 6 corresponds to two-photon resonance for the angle  $\Theta(\mathbf{p}_0) = 0.2$  rad and  $\chi_0 = 0.5$ . It is clearly seen Rabi oscillations of  $\mathcal{N}(p_0, t)$  with the mean period  $\mathcal{T}_R = 22\mathcal{T}$  ( $\mathcal{T}$  is the wave period). Rabi oscillations for three-photon resonance is displayed in Fig. 7 for the

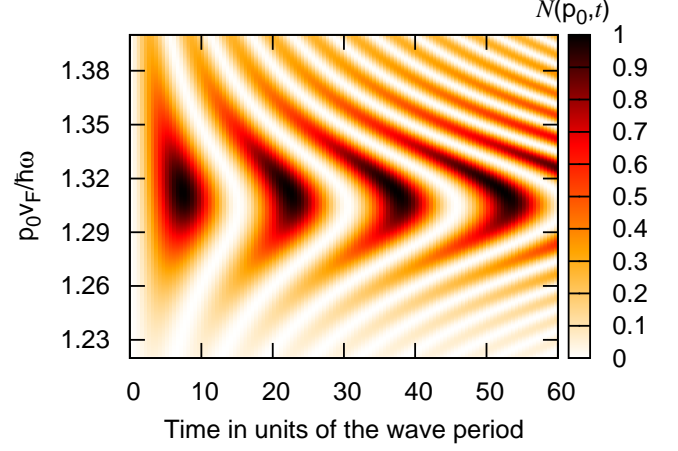


FIG. 7: (Color online) Same as Fig. 6, but for three-photon resonance ( $n = 3$ ). The angle is taken to be  $\Theta(\mathbf{p}_0) = \pi/2$  rad. The electric field dimensionless parameter is  $\chi_0 = 1.0$ .

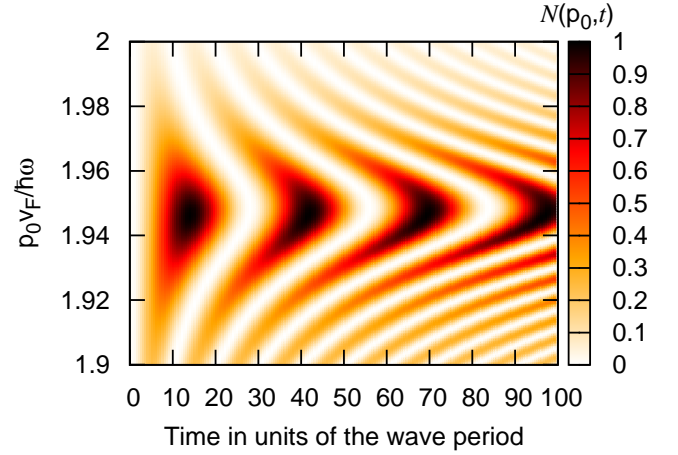


FIG. 8: (Color online) Four-photon resonance ( $n = 4$ ). Same as Fig. 7, but for the angle  $\Theta(\mathbf{p}_0) = 0.6$  rad. The electric field dimensionless parameter is  $\chi_0 = 1.0$ .

angle  $\Theta(\mathbf{p}_0) = \pi/2$  rad and  $\chi_0 = 1$ . Here mean Rabi period is  $\mathcal{T}_R = 15\mathcal{T}$ . Four-photon resonant Rabi oscillations with the mean period  $\mathcal{T}_R = 28\mathcal{T}$ , at the angle  $\Theta(\mathbf{p}_0) = 0.6$  rad is shown in Fig. 8.

To show the dependence of Rabi oscillations on the angle  $\Theta(\mathbf{p}_0)$ , in Figs. 9 and 10 colored 4D density plot of Rabi oscillations of the particle resonant distribution function  $\mathcal{N}_r(\mathbf{p}_0, t)$  on isosurfaces  $2\mathcal{E}_{E_0}(\mathbf{p}_0) / \hbar \omega = n$ , for  $n = 3, 4$  are shown at  $\chi_0 = 1$ . As is seen from these figures, for odd photon resonance the excited distribution function  $\mathcal{N}_r(\mathbf{p}_0, t)$  is maximal at the angle  $\Theta(\mathbf{p}_0) = \pi/2$  rad (perpendicular to applied electric field vector), while for even photon resonance at  $\Theta(\mathbf{p}_0) = \pi/2$  rad we have a minimum and main excitation takes place close to  $\Theta(\mathbf{p}_0) = \pi/4$ . The latter is connected with the fact that coupling term in Eqs. (30), (31) at

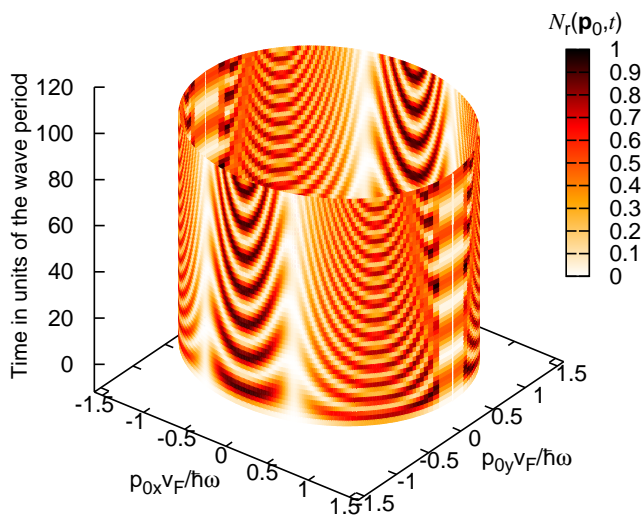


FIG. 9: (Color online) Colored 4D plot of Rabi oscillations of the particle distribution function  $\mathcal{N}_r(\mathbf{p}_0, t)$  for three-photon resonance on isosurface  $2\mathcal{E}_{E_0}(\mathbf{p}_0)/\hbar\omega = 3$ . The electric field dimensionless parameter is  $\chi_0 = 1.0$ .

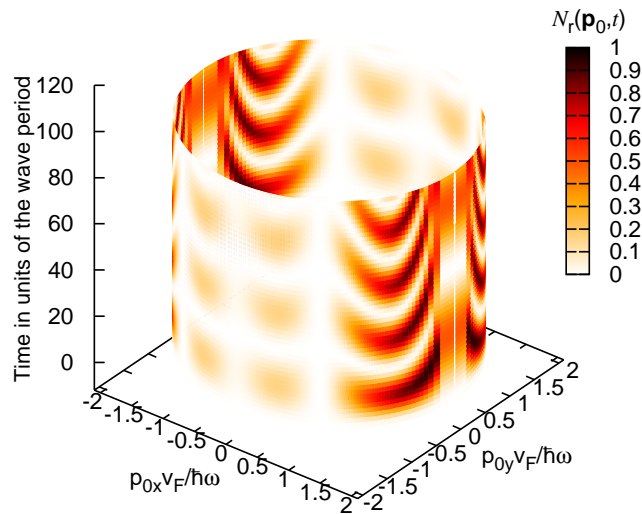


FIG. 10: (Color online) Same as Fig. 9, but for four-photon resonance:  $2\mathcal{E}_{E_0}(\mathbf{p}_0)/\hbar\omega = 4$ .

$\Theta(\mathbf{p}_0) = \pi/2$  rad contains only odd harmonics of the pump wave:  $G_{2s}(0, p_{0y}, E_0) = 0$ .

Summarizing, we see that numerical simulations are in agreement with analytical treatment in multiphoton resonant approximation and confirm simple physical picture described in previous section. We see that with laser fields of moderate intensities one can observe multiphoton excitation of Fermi-Dirac sea, the probabilities of which are comparable to and sometimes larger than one-photon excitation probability.

## V. CONCLUSION

We have presented a theoretical treatment of the coherent nonlinear response of a graphene under multiphoton interband excitation by a laser radiation. The evolutionary equation for single-particle density matrix is formulated arising from the second quantized formalism. The time-dependent single-particle density matrix in the given field of a laser radiation is calculated in the multiphoton resonant approximation. The Rabi oscillations of Fermi-Dirac sea at multiphoton excitation depending on the time, momentum, and photon number have been considered and analyzed also on the base of numerical simulations. The results obtained demonstrate that the Rabi oscillations of Fermi-Dirac sea corresponding to multiphoton excitation can already be observed for such laser fields where the work of electric field on the wave period is comparable to photon energy  $\varepsilon_\gamma = \hbar\omega$ . For mid-infrared lasers  $\varepsilon_\gamma \sim 0.1$  eV, multiphoton interaction regime can be achieved at the intensities  $I > 10^7$  W cm $^{-2}$ , for the time scales 1.0 ps. For near-infrared range of frequencies  $\varepsilon_\gamma \sim 1$  eV, multiphoton interaction regime can be achieved at the intensities  $I > 10^{11}$  W cm $^{-2}$ , for the time scales 100.0 fs.

## Acknowledgments

This work was supported by State Committee of Science (SCS) of Republic of Armenia (RA), Project No. 11RB-006.

\* Electronic address: avetissian@ysu.am

<sup>1</sup> K. S. Novoselov, A. K. Geim, S. V. Morozov, D. Jiang, Y. Zhang, S. V. Dubonos, I. V. Grigorieva, and A. A. Firsov, *Science* **306**, 666 (2004).

<sup>2</sup> A. H. Castro Neto, F. Guinea, N. M. R. Peres, K. S. Novoselov, and A. K. Geim, *Rev. Mod. Phys.* **81**, 109 (2009).

<sup>3</sup> A. K. Geim, *Science* **324**, 1530 (2009).

<sup>4</sup> K.S. Novoselov, A. K. Geim, S. V. Morozov, D. Jiang, M.

I. Katsnelson, I. V. Grigorieva, S.V. Dubonos and A. A. Firsov, *Nature*, **438**, 197 (2005).

<sup>5</sup> G. W. Semenoff, *Phys. Rev. Lett.* **53**, 2449 (1984).

<sup>6</sup> F. D. M. Haldane, *Phys. Rev. Lett.* **61**, 2015 (1988).

<sup>7</sup> M. I. Katsnelson, K. S. Novoselov, and A. K. Geim, *Nature Phys.* **2**, 620 (2006).

<sup>8</sup> V. V. Cheianov, V. I. Fal'ko, and B. L. Altshuler, *Science* **315**, 1252 (2007).

<sup>9</sup> M. I. Katsnelson and K. S. Novoselov, *Solid State Com-*



- mun. **143**, 3 (2007).
- <sup>10</sup> H.K. Avetissian, *Relativistic Nonlinear Electrodynamics* (Springer, New York, 2006).
- <sup>11</sup> M.I. Katsnelson, *Materials Today* **10**, 20 (2007).
- <sup>12</sup> V. V. Cheianov and V. I. Fal'ko, *Phys. Rev. B* **74**, 041403 (2006).
- <sup>13</sup> C. W. J. Beenakker, *Rev. Mod. Phys.* **80**, 1337 (2008).
- <sup>14</sup> C. Itzykson, J. -B. Zubar, *Quantum Field Theory* (Dover, 2006).
- <sup>15</sup> M. I. Katsnelson, *Eur. Phys. J. B* **51**, 157 (2006).
- <sup>16</sup> J. Cserti and Gy. Dávid, *Phys. Rev. B* **74**, 172305 (2006).
- <sup>17</sup> J. Schliemann, *New J. Phys.* **10**, 043024 (2008).
- <sup>18</sup> J. Schwinger, *Phys. Rev.* **82**, 664 (1951).
- <sup>19</sup> D. Allor, T. D. Cohen, D. A. McGady, *Phys.Rev. D* **78**, 096009 (2008).
- <sup>20</sup> B. Dóra and R. Moessner, *Phys. Rev. B* **81**, 165431 (2010).
- <sup>21</sup> A.W. W. Ludwig, M. P. A. Fisher, R. Shankar, and G. Grinstein, *Phys. Rev. B* **50**, 7526 (1994).
- <sup>22</sup> K. Ziegler, *Phys. Rev. B* **75**, 233407 (2007).
- <sup>23</sup> H. K. Avetissian, A. K. Avetissian, G. F. Mkrtchian, Kh. V. Sedrakian, *Phys. Rev. E* **66**, 016502 (2002).
- <sup>24</sup> L. Allen, J. H. Eberly, *Optical Resonance and Two Level Atoms* (Wiley-Interscience, New York, 1975); B.W. Shore, *Theory of Coherent Atomic Excitation* (Wiley-Interscience, New York, 1990); M. O. Scully and M. S. Zubairy, *Quantum Optics* (Cambridge University Press, Cambridge, U.K., 1997).
- <sup>25</sup> F. Rossi and T. Kuhn, *Rev. of Mod. Phys.*, 74, 895 (2002); V. M. Axt and T. Kuhn, *Rep. Prog. Phys.* 67, 433 (2004).
- <sup>26</sup> E. G. Mishchenko, *Phys. Rev. Lett.* **103**, 246802 (2009).
- <sup>27</sup> P.N. Romanets and F.T. Vasko, *Phys. Rev. B* **81**, 241411(R) (2010).
- <sup>28</sup> B. Dóra, K. Ziegler, P. Thalmeier, and M. Nakamura, *Phys. Rev. Lett.* **102**, 036803 (2009).
- <sup>29</sup> H. K. Avetissian, G. F. Mkrtchian, *Phys. Rev. A* **66**, 033403 (2002).
- <sup>30</sup> H. K. Avetissian, B. R. Avchyan, and G. F. Mkrtchian, *Phys. Rev. A* **77**, 023409 (2008).
- <sup>31</sup> H. K. Avetissian, B. R. Avchyan, G. F. Mkrtchian, *Phys. Rev. A* **82**, 063412 (2010).